Chapter 12
Nuclear Matter Properties at High Densities: Squeezing Out Nuclear Matter Properties from Experimental Data

Yvonne Leifels

Abstract The nuclear equation of state is a topic of highest current interest in nuclear physics and astrophysics. The nuclear equation of state governs the evolution of heavy-ion reactions as well as the characteristics of compact stellar objects like neutron stars, the explosions of supernovae, and the merging of two neutron stars. The symmetry energy is the part of the equation of state which is connected to the asymmetry in the neutron/proton content. During recent years a multitude of experimental and theoretical efforts on different fields have been undertaken to constraint its density dependence at low densities but also above saturation density ($\rho_0 = 0.16\text{fm}^{-3}$). Conventionally, the symmetry energy is described by its magnitude S_v and the slope parameter L, both at saturation density. Values of $L \approx 44$–66 MeV and $S_v \approx 31$–33 MeV have been deduced in recent compilations of nuclear structure, heavy-ion reaction, and astrophysics data. Apart from astrophysical data on mass and radii of neutron stars and the gravitational wave signal of neutron star mergers, heavy-ion reactions above incident energies of several 100 MeV are the only means to access the high-density behavior of the symmetry energy. In particular, meson production and collective flows up to about 1 GeV/nucleon are predicted to be sensitive to the slope of the symmetry energy as a function of density. From the measurement of elliptic flow of neutrons with respect to charged particles at GSI, a stringent constraint for the slope of the symmetry energy at supra-saturation densities has been deduced. Future options to reach even higher densities will be discussed.

Y. Leifels (✉)
GSI Helmholtzzentrum für Schwerionenforschung, Planckstr. 1, 64291 Darmstadt, Germany
e-mail: y.leifels@gsi.de

R. K. Puri et al. (eds.), *Advances in Nuclear Physics*, Springer Proceedings in Physics 257, https://doi.org/10.1007/978-981-15-9062-7_12

12.1 Introduction

The nuclear matter equation of state (EOS) is one of central topics in nuclear physics. It defines the evolution of nuclear reactions and the characteristics of compact stars and cataclysmic astrophysical events like supernova explosions and neutron star mergers. A theoretical determination of the nuclear EOS from first principles by microscopic calculations using realistic two and three-body nuclear interactions is highly non-trivial and a subject of current scientific research using different approaches, i.e., quantum many-body theory in the Brueckner-Hartree-Fock approximation or chiral perturbation theory (ChPT). From astrophysical observations meaningful constraints can be obtained to the nuclear EOS, however, heavy-ion collisions are the only means to study the characteristics of the nuclear EOS in the laboratory.

The nuclear EOS describes the relation between density, pressure, energy, temperature, and the isospin asymmetry $\delta = (\rho_n - \rho_p)/\rho$, where ρ_n, ρ_p, and ρ are neutron, proton, and nuclear matter densities, respectively. It is conventionally divided into a symmetric matter part independent of the isospin asymmetry and an isospin term, also quoted as symmetry energy $E_{sym}(\rho)$, that enters with a factor δ^2 into the equation of state. In this description, the symmetry energy is the difference in the energy between symmetric matter $\rho_n = \rho_p$ and pure neutron matter. Different density dependencies of $E_{sym}(\rho)$ can be described quantitatively by expanding the symmetry energy in terms of $(\rho - \rho_0)/\rho_0$ using the value of $E_{sym,0} = E_{sym}(\rho = \rho_0)$ and the slope parameter at normal nuclear matter density $L = 3\rho_0 \frac{\delta E_{sym}(\rho)}{\delta \rho}|_{\rho=\rho_0}$ leading to the following equation:

$$E_{sym}(\rho) = E_{sym,0} + \frac{L}{3}\left(\frac{(\rho - \rho_0)}{\rho_0}\right) + \frac{K_{sym}}{18}\left(\frac{(\rho - \rho_0)}{\rho_0}\right)^2 + ...,$$

where K_{sym} is referred to as curvature parameter.

Microscopic calculations of the energy functional of nuclear matter employing different approaches to the nucleon-nucleon interaction predict rather different forms of the EOS. Most calculations for the symmetry energy coincide at or slightly below normal nuclear matter density (compare Fig. 12.5 right panel), which demonstrates that constraints from finite nuclei are active for an average density smaller than saturation density and surface effects play a role. In contrast to that extrapolations to supra-normal densities diverge dramatically. The density dependence of the nuclear symmetry energy is an important constituent for drip lines, masses, densities, and collective excitations of neutron-rich nuclei [1], flows,m and multi-fragmentation in heavy-ion collisions at intermediate energies [2, 3], but also for astrophysical phenomena like supernovae, neutron stars [4], and the merging of two neutron stars [5], which have been recently observed and identified by the characteristic gravitational wave signal and the simultaneous emission of γ-rays.

Many results of nuclear structure and nuclear reaction measurements as well as astrophysical observations have been collected in [6]. The symmetry energy $E_{sym,0}$ and the slope parameter L at saturation density have been deduced to be

$E_{sym,0} = 31.6 \pm 2.7$ MeV and $L = 59 \pm 16$ MeV, despite the quite large variations in the individual measurements. However, L and $E_{sym,0}$ cannot be individually determined in most experiments, often a larger value of L is compensated by a smaller $E_{sym,o}$ or vice versa.The authors of [7] have extracted experimental constraints from nuclear physics and astrophysical measurements in the $E_{sym,0}$–L plane, which give a consensus region of 40 MeV $< L(\rho_0) <$ 60 MeV and 30 MeV $< E_{sym,0} <$ 32 MeV with 68 % confidence, which is in mutual agreement with the results quoted in [6]. However, in another publication [8] it was argued, while using isobaric analog states and isovector skins on neutron-rich nuclei, that both symmetry parameters may be larger than the commonly adopted values.

The symmetry energy at higher densities $\rho > \rho_0$ can be accessed by the determination of the mass and the radii of neutron stars [9] or by investigating observables in heavy-ion collisions which are related to the early, high-density phase of the reactions and its isospin content. Theoretical model calculations predict that for a short time period of 20 fm/c densities up to 3 ρ_0 are reached in the central zone of a heavy-ion collision even at moderate energies $\approx$ 1 GeV/nucleon [2]. At lower energies around 200 MeV/nucleon up to $2\rho/\rho_0$ may still be reached. However, one should be aware that the highest density reached during a heavy-ion collision is not necessarily equivalent to the density which is probed by a certain observable. This question has to be addressed when extracting constraints on the density dependence of the symmetry energy from experimental data.

A multitude of observables have been proposed to be sensitive to the symmetry energy (for a review see [2]): ratio of multiplicities or spectra of isospin partners (e.g., π^-/π^+, n/p or t/^{3}He) and the comparison of their flows: The ratio of positively and negatively charged pions measured close to or below the production threshold in the NN system ($E_{beam,thr} = 280$ MeV) is one of the observables discussed. It is predicted to be sensitive to the density dependence of the symmetry energy. Indeed, model predictions obtained with the transport code IBUU4 [11] could only reproduce existing experimental data on pion production around $E_{beam} = 400$ MeV/nucleon in various collisions systems [12] when a rather soft density dependence of the symmetry energy was applied. Incorporation of in-medium effects in addition to the symmetry energy, like, e.g., pion potentials, s-wave production of pions, and the properties of intermediate Delta resonances, may lead to different and even opposite conclusions [13, 14], while describing the experimental data equally well. It is still not settled how the symmetry energy influences the pion production ration. An experimental way out is to measure double ratios of pion production, i.e., compare pion production in a neutron-rich and proton-rich system having the same Z. Here, some input parameters to the models will drop out. Such experiments have been accomplished at the Riken facility with the BIGRIPS magnet and the SPIRIT TPC, recently.

Other observables sensitive to the symmetry energy at supra-normal densities are collective flows. At energies below 1 GeV/nucleon the reaction dynamics is largely determined by the nuclear mean field. The resulting pressure produces a collective motion of the compressed material whose strength will be influenced by the symme-

try energy in isospin-asymmetric systems. The FOPI collaboration has measured a multitude of flow observables in many different collisions systems [15] in the energy regime between 200 and 2000 MeV/nucleon with FOPI setup at SIS18@GSI.

12.2 Neutron and Charged Particle Elliptic Flow

The strengths of collective flows in heavy-ion collisions are determined by a Fourier expansion of the azimuthal distributions of particles around the reaction plane:

$$\frac{d\sigma(y)}{d\phi} = C(1 + 2v_1(y)\cos\phi + 2v_2(y)\cos 2\phi.....) \tag{12.1}$$

The side flow of particles is characterized by the coefficient v_1 and the elliptic flow by v_2. The value of v_2 around mid-rapidity is negative at incident beam energies between 0.2 and 6 GeV/nucleon which signifies that matter is squeezed out perpendicular to the reaction plane. Elliptic flow at those energies is known to be sensitive to the stiffness of the symmetric part of the nuclear equation of state. In Fig. 12.1 data of (negative) elliptic flow of protons is shown for mid-central Au+Au collisions at 400 MeV/nucleon (left panel) and 1.2 GeV/nucleon (right panel). The bell-shaped experimental data are compared to IQMD predictions [16] employing a soft (SM) and hard (HM) density dependence of the nuclear matter equation of state. The particles within IQMD are interacting via a momentum dependent interaction which has been deduced from experimental data on proton scattering off nuclei [16]. A momentum dependent interaction is needed to describe the energy dependence of flow and pion

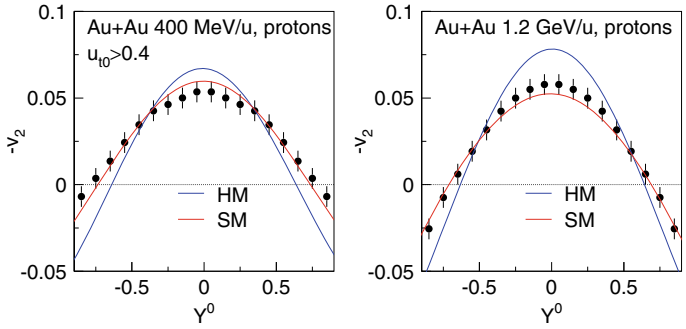

Fig. 12.1 The elliptic flow v_2 measured with the FOPI setup in semi-central Au+Au collisions as function of normalized rapidity $Y^0 = y/y_p$, where y is the particle rapidity in the center-of-mass system and y_p the rapidity of the projectile. The initial target-projectile rapidity gap always extends from $Y^0 = -1$ to $Y^0 = 1$. The experimental data (shown as block points) are compared to IQMD predictions [16] employing a soft EOS (denoted as red line) and a hard EOS (blue line). The calculations have been performed using a momentum dependent interaction. Data and calculations are taken from [15, 17]

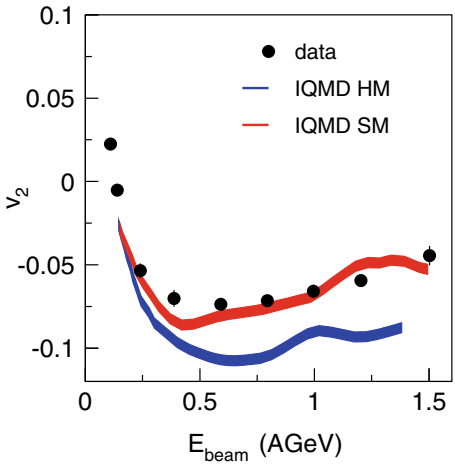

Fig. 12.2 Elliptic flow v_2 of protons as a function of beam energy for Au+Au collisions and semi-central collisions [15]. The data points are shown as full circles, predictions of the IQMD model for a soft and a hard nuclear equation of state with momentum dependent interactions by red and blue bands, respectively. Particles around mid-rapidity ($|Y^0| < 0.2$) and with high transverse momenta ($u_t^0 > 0.8$) are selected. u_t is the transverse component of the four-velocity u, $u_t = \beta_t \gamma$, where $u_t^0 = u_t/u_p$, with $u_p = \beta_p \gamma_p$, the index p referring to the incident projectile in the center-of-mass system [15, 16]

production data simultaneously. Clearly, a soft density dependence of the nuclear EOS is needed to describe the experimental data at both energies. Not only the size of the elliptic flow v_2 at mid-rapidity is described but also the rapidity dependence of v_2, which supports in addition the choice of the specific input parameters to the transport model, which is in addition constraint by other experimental results of the FOPI collaboration.

Data for the elliptic flow v_2 of protons emitted around mid-rapidity in semi-central Au+Au collisions [15] as a function of beam energy together with predictions of the IQMD model for HM and SM nuclear equation of state augmented by a momentum dependent interaction are shown in Fig. 12.2. Again, the experimental data are best described by calculations utilizing a soft (SM) equation of state. The larger negative v_2-values for a hard equation of state are almost completely due to the higher density gradients perpendicular to the reaction plane and, therefore, an effect of the acting potentials [17].

The ratio of elliptic flow strengths of neutrons and light charged particles has been proposed by using a version of the UrQMD transport code [18] as a robust observable sensitive to the EOS of asymmetric matter [19]. Neutron and proton emission has been already measured by a combination of the LAND neutron detector with a part of the FOPI setup [20]. A reanalysis of the data and comparison to the results of the UrQMD transport model [19] yielded a moderately soft symmetry energy dependence on density, $L = 86 \pm 15$ MeV. Despite the large error a particular soft

or a very stiff density dependence of the symmetry energy could ruled out. These results have been confirmed by using a different transport code [21]. Nevertheless, the statistical error bars of the data are rather large, and, therefore, an attempt was started by the ASY-EOS collaboration to remeasure neutron/proton flow in Au+Au collisions at an incident energy $E_{beam} = 400$A MeV.

12.2.1 The ASY-EOS Experiment

The setup of the ASY-EOS experiment at the SIS18 accelerator is presented in Fig. 12.3. Upstream from the target, a thin plastic scintillator foil was placed for measuring the beam particles and serving as a start detector for the time-of-flight systems. The granular and high-efficient neutron detector LAND was placed close to 45° with respect to the beam direction. A veto wall of thin plastic scintillator material in front of LAND was used to discriminate between neutrons and charged particles. The Krakow Tripple Telescope Array (KRATTA was placed opposite to LAND covering approximately the same angular acceptance. This device allows to identify light charged fragments. Three detector systems were used for event characterization and background suppression. The ALADIN Time-of-Flight (ATOF) detected

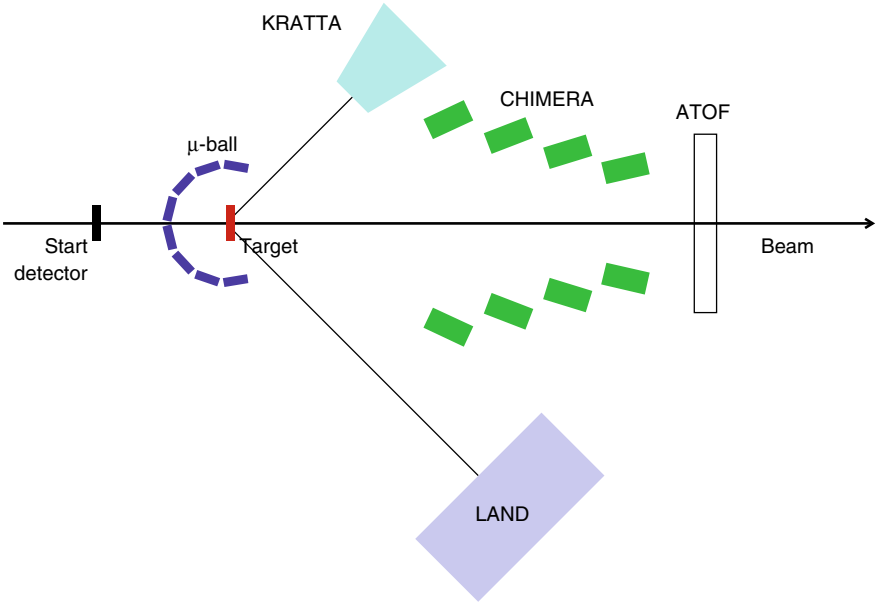

Fig. 12.3 Sketch of the setup of the ASY-EOS experiment (S394) at the SIS18 of GSI showing the six main detector systems and their positions relative to the beam direction. Dimensions and distances are not to scale (from [22])

charged particles and fragments emitted at very small polar angles $\Theta_{lab} < 7°$ close to thebeam. Four double rings of the CHIMERA multidetector consisting out of 352 CsI(Tl) scintillators were placed in forward direction, and the target was surrounded by four rings with 50 thin CsI(Tl) elements of the Washington University Microball array. Those detectors provided sufficient granularity and solid angle coverage to determine the orientation of the reaction plane and the impact parameter. A detailed description of the setup is available in [22].

12.2.2 Experimental Results

The data analysis procedure is described in detail in [22]. The v_2 ratios obtained for neutrons v_2^n and light charged particles v_2^{ch} after applying all corrections are shown in Fig. 12.4. Constraints to the symmetry energy were obtained by comparing the ratio v_2^n/v_2^{ch} with corresponding UrQMD predictions.

A soft iso-scalar EOS was chosen for the calculations and the following parameterization was used for the density dependence of the symmetry energy:

$$E_{sym}(\rho) = E_{sym}^{pot}(\rho) + E_{sym}^{kin}(\rho) = 22\text{MeV}(\rho/\rho_0)^{\gamma} + 12(\rho/\rho_0)^{2/3}\text{MeV}, \quad (12.2)$$

with $\gamma = 0.5$ and $\gamma = 1.5$ corresponding to a soft and a stiff density dependence, respectively.

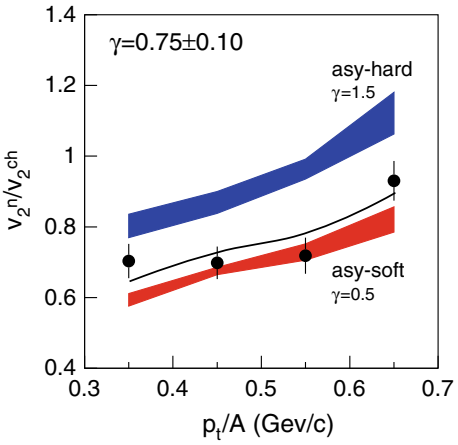

Fig. 12.4 Elliptic flow ratio of neutrons over charged particles measured in the same acceptance range for central ($b < 7.5$ fm) Au+Au collisions at 400 MeV/nucleon as a function of transverse momentum, p_t/A. The black circles represent the experimental data. The blue and red bands represent the results of UrQMD model calculations employing a hard and soft density dependence of the symmetry energy. Fitting a linear interpolation between the two extremes to the experimental data yields a γ-value of $\gamma = 0.75 \pm 0.10$. The black line shows the resulting predictions

The two predictions obtained under these conditions are presented in Fig. 12.4 together with the experimental results. The parameters which describe the data best are obtained by fitting a linear interpolation between the two predictions. The resulting power-law coefficient is $\gamma = 0.75 \pm 0.10$. The corresponding v_2 ratio is shown as black line in Fig.12.4. In comparison with the FOPI-LAND data, the statistical accuracy of the ASY-EOS experiments represents an improvement by a factor of 2. A systematic uncertainty arose from occasional malfunction of the electronic circuits for the time measurement with LAND. It prohibits extending the data evaluation into the region of large transverse momenta. For this reason this analysis is restricted to $p_t < 0.7$ GeV/c. Another uncertainty is related to the lower energy threshold for neutron detection. The necessary corrections and the methods used for estimating the remaining errors are described in detail in [22].

With all corrections and errors included, the acceptance-integrated elliptic flow values lead to a power-law coefficient $\gamma = 0.72 \pm 0.19$. The corresponding slope value is $L = 72 \pm 13$ MeV. Changing the absolute value of the symmetry energy at ground state nuclear matter density in the simulations to a lower value, $E_{sym}(\rho_0) =$ 31MeV, results in a lower γ-value $\gamma = 0.68 \pm 0.19$. This is still within the error bar of the above result.

This result is displayed in Fig. 12.5 (right panel) where the symmetry energy is shown as a function of reduced density ρ/ρ_0 together with various microscopic model predictions [23]. The experimental data are represented as colored bands. The results of the FOPI-LAND experiment are shown in yellow and the one of the ASY-Experiment in orange. For completeness the calculations from [23] for the EOS of symmetric matter are shown in the left panel of Fig. 12.5 together with the experimental constraint from the FOPI collaboration [17] utilizing elliptic flow of protons and light charged particles in Au+Au collisions between 0.25 and 1.5 GeV/nucleon.

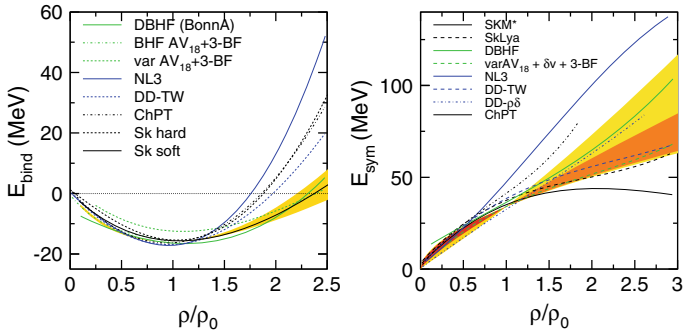

Fig. 12.5 Left panel: Constraints from experimental data of the FOPI collaboration as presented in [17] (yellow area) are shown together with predictions of microscopic model calculations employing different methods and different interactions [23]. Right panel: Result of the ASY-EOS experiment (orange area) and the FOPI-LAND analysis (yellow area) together with theoretical predictions for $E_{sym}(\rho)$ using different microscopic approaches in addition to Skyrme interactions. The calculations are taken from [23]

12.2.3 Density Tested in the ASY-EOS Experiment

Since microscopic transport models are reproducing reasonably well the experimental data it seems to be appropriate to deduce the density range relevant for the sensitivity to the symmetry energy in this reaction by using one of those codes. For this investigation the Tübingen Version of the QMD model, TüQMD, [21] was chosen (see [22] for more details). The two density dependencies of the symmetry energy, hard and soft (blue and red lines in Fig. 12.6, respectively), are shown in the left panel of Fig. 12.6 together with the linear form (black line) used as default parameterization. To quantify the results, the function $DERF$ (Difference of elliptic flow ratio) is defined:

$$DERF^{n,Z}(\rho) = \frac{v_2^n}{v_2^Z}(hard, \rho) - \frac{v_2^n}{v_2^Z}(soft, \rho). \tag{12.3}$$

An example of the function $DERF(\rho)$ is presented in the middle panel of Fig. 12.6. At zero density $DERF(0)$ is zero by definition and at high densities $DERF(\rho)$ is approaching the maximal value, which is the variation of v_2 for the two options of E_{sym}. The region in density where $DERF(\rho)$ is changing most rapidly is also the density regime which is most relevant for the determination of the symmetry energy. Hence, the value of the derivative $\mathrm{d}DERF(\rho)/\mathrm{d}\rho$ is a measure of the impact of the symmetry energy on the elliptic flow observables. In the right panel of Fig. 12.6 the derivative of $DERF(\rho)$ is shown for three choices of the elliptic flow ratio: For protons (n/p), hydrogen isotopes (n/H) and all charged particles (n/ch).

It can be seen in the figure that the maximum sensitivity achieved with the elliptic flow ratio of neutrons to charged particles is reached close to saturation density and extends beyond twice this value. This finding is in agreement with results of [17] which were obtained by analyzing also elliptic flow data of charged particles and

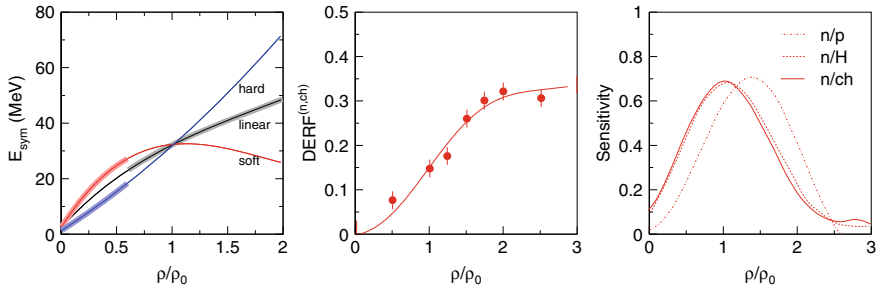

Fig. 12.6 Left panel: The different parameterizations describing the density dependence of the symmetry energy which were used for the investigation described in the text. The linear one was employed as a normal or default form of $E_{sym}(\rho)$. Middle panel: The function $DERF(\rho)$ for the ratio of elliptic flows of neutrons and charged particles. Right panel: Derivative of $DERF(\rho)$ as a function of density for different particle choices. These results are taken from [22]

using the IQMD model [16]. For $^{197}Au + Au$ collisions at 400 MeV/u the force-weighted density, defined by the authors, is spread over a broad density regime extending from $0.8 < \rho/\rho_0 < 1.6$.

The derivative of $DERF(\rho)$ for the neutron-proton ratio peaks at a higher value, 1.4 to $1.5\rho_0$. This observation gives rise to the expectation that with sufficient isotope separation one would be able not only to constraint the slope of the symmetry energy but also its curvature.

12.3 Conclusions and Outlook

The symmetry energy at supra-saturation densities can be effectively probed with the elliptic flow ratio of neutrons and charged particles. The ASY-EOS collaboration measured data for Au+Au collisions at 400A MeV, and a slope for the of $L = 72 \pm 13$ for the density dependence of the symmetry energy could be deduced from the v_2 ratio of neutrons and charged particles. According to model predictions, similar observables might also be sensitive not only to the slope of the symmetry energy but also to its curvature at high densities. Hence, it would be interesting to measure n and light charged particle flow also at higher energies and for different systems. In collisions of Sn-isotopes one could investigate the evolution of the v_2 ratio as a function of N/Z of the colliding system.

How the sensitivity of the various observables to the symmetry energy develops with rising beam energy and larger densities is by no means obvious and more calculations using different models and prescriptions need to be performed. Particle production is predicted to be most sensitive to modifications in the neutron/proton density close to threshold. Kaon production below and close to threshold ($E_{thr,NN} = 1.6$ GeV has proven to be sensitive to the density reached in the course of the collision. It has been shown in particular that Kaon yields are robust observables to constrain the iso-scalar EOS [24]. At sub-threshold energies Kaons are produced in the central high-density region and, because they are not re-absorbed by the surrounding nuclear matter, they are true messengers of the dense overlap zone. The production ratio (K^+/K^0) is predicted to be sensitive to the symmetry energy and, therefore, may be an interesting observable accessing densities beyond twice saturation density. An experiment studying Au+Au reactions at 1.25A GeV was performed by the HADES collaboration. The HADES detector setup allows not only for measuring charged Kaons but also reconstructing K^0 by their decay into charged pions with high accuracy. Sufficient statistic was accumulated and the data have been published and compared to predictions of transport models. However, the sensitivity to the symmetry energy has not yet been tested.

Symmetry effects are very small, because the contribution of the symmetry energy enters with a factor δ^2 into the equation of the state of nuclear matter. Since δ is rather small even for the most neutron-rich stable isotopes it is evident that those studies have to be extended to radioactive beams with enhanced neutron-proton asymmetry. Experimental facilities, e.g., RIKEN/RIBF, MSU/FRIB, GANIL/SPIRAL2 are

or will become available, which allow further studies of the symmetry energy by different experimental methods. But the highest energies and consequently highest densities will be accessed with FAIR/Super-FRS facility. The super fragment separator Super-FRS will have a magnetic rigidity of 20 Tm and will provide radioactive beams up to 1 GeV/nucleon. This will offer the possibility to study the symmetry energy at high densities. Nevertheless, the neutron-proton asymmetry which may be accessed in such experiments is not significantly larger than the one reached in Au+Au or Pb+Pb collisions with the concomitant disadvantage that the collision systems are getting smaller and the densities reached in the course of the reactions are not as large as in the heavy Au-system. Hence, for flow and particle production observables it may not be necessary to utilize radioactive beams, and stable beams and targets would be sufficient. In such case, it would be impossible to generate double ratios in order to diminish systematic errors in the experiment and uncertainties due to unknown input parameters to the models. This would require sophisticated transport codes which have been benchmarked intensively to experimental data (see [25] for an ongoing effort in comparing different transport codes).

Acknowledgements Results presented in this contribution have been obtained within the ASY-EOS collaboration. See [22] for a complete list of authors.

References

1. B.A. Brown, Neutron radii in nuclei and the neutron equation of state. Phys. Rev. Lett. **85**, 5296 (2000); X. Roca-Maza, M. Centelles, X. Viñas, M. Warda, Neutron skin of ^{208}Pb, nuclear symmetry energy, and the parity radius experiment. Phys. Rev. Lett. **106**, 252501 (2011)
2. B.-A. Li, L.-W. Chen, C.M. Ko, Recent progress and new challenges in isospin physics with heavy-ion reactions. Phys. Rep. **464**, 113–281 (2008)
3. B. Tsang et al., Constraints on the density dependence of the symmetry energy. Phys. Rev. Lett. **102**, 122701 (2009)
4. A.W. Steiner et al., Isospin asymmetry in nuclei and neutron stars. Phys. Rep. **411**, 325–375 (2005)
5. A. Bauswein et al. Identifying a first-order phase transition in neutron-star mergers through gravitational waves. Phys. Rev. Lett. **122**, 061102 (2019)
6. B.-A. Li, X. Han, Constraining the neutron-proton effective mass splitting using empirical constraints on the density dependence of nuclear symmetry energy around normal density. Phys. Lett. B **727**, 276–281 (2013)
7. I. Tews et al., Symmetry parameter constraints from a lower bound on neutron-matter energy. Astro. Phys. J. **848**, 1 (2017)
8. P. Danielewicz et al., Symmetry energy III: Isovector skins. Nucl. Phys. A **958**, 147–186 (2017)
9. J.M. Lattimer, A. Steiner, Constraints on the symmetry energy using the mass-radius relation of neutron stars. Eur. Phys. J. A **50**, 40 (2014)
10. B.A. Brown, Constraints on the Skyrme equations of state from properties of doubly magic nuclei. Phys. Rev. Lett. **111**, 232502 (2013)
11. Z. Xiao et al., Circumstantial evidence for a soft nuclear symmetry energy at suprasaturation densities. Phys. Rev. Lett. **102**, 062502 (2009)
12. W. Reisdorf et al., Systematics of pion emission in heavy ion collisions in the 1AGeV regime. Nucl. Phys. A **781**, 459–508 (2007)

13. Z.Q. Feng, G.M. Jin, Probing high-density behavior of symmetry energy from pion emission in heavy-ion collisions. Phys. Lett. B **683**, 140–144 (2010)
14. J. Hong, P. Danielewicz, Subthreshold pion production within a transport description of central Au + Au collisions. Phys. Rev. C **90**, 024605 (2014)
15. W. Reisdorf et al., Systematics of azimuthal asymmetries in heavy ion collisions in the 1AGeV regime. Nucl. Phys. A **876**, 1–60 (2012)
16. Ch. Hartnack et al., Modelling the many-body dynamics of heavy ion collisions: present status and future perspective. Eur. Phys. J. A **1**, 151–169 (1998)
17. A. Le Fèvre et al., Constraining the nuclear matter equation of state around twice saturation density. Nucl. Phys. A **945**, 112–133 (2016)
18. Q. Li, M. Bleicher, H. Stocker, The effect of pre-formed hadron potentials on the dynamics of heavy ion collisions and the HBT puzzle. Phys. Lett. B **659**, 525–530 (2008)
19. P. Russotto et al., Importance of nuclear effects in the measurement of neutrino oscillation parameters. Phys. Lett. B **697**, 471–476 (2011)
20. Y. Leifels et al., Exclusive studies of neutron and charged particle emission in collisions of ^{197}Au + ^{197}Au at 400 MeV/nucleon. Phys. Rev. Lett. **71**, 963–966 (1993)
21. M.D. Cozma, Neutron-proton elliptic flow difference as a probe for the high density dependence of the symmetry energy. Phys. Lett. B **700**, 139–144 (2011)
22. P. Russotto et al., Results of the ASY-EOS experiment at GSI: The symmetry energy at suprasaturation density. Phys. Rev. C **94**, 034608 (2016)
23. C. Fuchs, H.H. Wolter, Modelization of the EOS. Eur. Phys. J. A **30**, 5–21 (2006)
24. Ch. Hartnack et al., Hadronic matter is soft. Phys. Rev. Lett **96**, 012302 (2006)
25. O. Akira et al., Comparison of heavy-ion transport simulations: collision integral with pions and δ resonances in a box (2019), arXiv:1904.02888v2 [nucl-th]